Structure of Isocitrate Dehydrogenase with α-Ketoglutarate at 2.7-Å Resolution: Conformational Changes Induced by Decarboxylation of Isocitrate†

Barry L. Stoddard‡ and Daniel E. Koshland, Jr.*

Department of Molecular and Cellular Biology, Division of Biochemistry, 229 Stanley Hall, University of California, Berkeley, California 94720

Received December 15, 1992; Revised Manuscript Received May 13, 1993®

ABSTRACT: The structure of the isocitrate dehydrogenase (IDH) complex with bound α-ketoglutarate, Ca^{2+}, and NADPH was solved at 2.7-Å resolution. The α-ketoglutarate binds in the active site at the same position and orientation as isocitrate, with a difference between the two bound molecules of about 0.8 Å. The Ca^{2+} metal is coordinated by α-ketoglutarate, three conserved aspartate residues, and a pair of water molecules. The largest motion in the active site relative to the isocitrate enzyme complex is observed for tyrosine 160, which originally forms a hydrogen bond to the labile carboxyl group of isocitrate and moves to form a new hydrogen bond to Asp 307 in the complex with α-ketoglutarate. This triggers a number of significant movements among several short loops and adjoining secondary structural elements in the enzyme, most of which participate in dimer stabilization and formation of the active-site cleft. These rearrangements are similar to the ligand-binding-induced movements observed in globins and insulin and serve as a model for an enzymatic mechanism which involves local shifts of secondary structural elements during turnover, rather than large-scale domain closures or loop transitions induced by substrate binding such as those observed in hexokinase or triosephosphate isomerase.

Many enzymes undergo substrate-induced conformational changes in response to binding of ligand. These motions are varied and may function to orient catalytic groups around the substrate, stabilize the transition state, align orbitals for efficient electron transfer, maintain substrate specificity, and/or exclude water from the active site during catalysis. Many enzymes have been shown crystallographically to exhibit substrate-induced motions ranging from large-scale domain closure to loop conformational transitions to more subtle shifting and repacking of secondary structural elements, indicating that induced fit rather than templatelike behavior is the norm for enzyme action. There are, however, some enzymes which show small substrate-induced conformational changes upon binding, including, for example, serine proteases and ribonuclease. A possibility exists that some or all of these enzymes may depend on conformational motions during catalysis which are not detected by the examination of an initial enzyme/substrate complex. Isocitrate dehydrogenase (IDH) seems to fall in this category, and therefore a closer examination of its conformation during catalysis seemed appropriate.

The structure of IDH has been solved at 2.5-Å resolution in the forms of apoenzyme, phosphorylated apoenzyme, a binary complex of isocitrate and Mg^{2+}, complexed to $NADP^+$ in the absence of substrate and metal (Hurley *et al.*, 1989, 1990a,b, 1991), and in a ternary complex with isocitrate, $NADP^+$, and Ca^{2+}, which serves as a model for the initial bound Michaelis complex (Stoddard *et al.*, 1993). All of these structures display remarkably similar protein conformations, with rms differences in backbone positions of 0.2–0.5 Å and little movement of protein backbone atoms of greater than approximately 1 Å. The enzyme is a dimer of 416 residues per subunit and contains a single catalytic metal per monomer which is tightly chelated by two conserved aspartate residues and by bound isocitrate (Hurley *et al.*, 1990b). The substrate molecule is bound in the active site primarily through interactions between its free carboxylate groups and several conserved basic residues (Figure 1). Steady-state kinetic studies of IDH, in addition to product inhibition studies and examination of turnover using alternative substrate and metal species, indicate that the enzyme possesses a steady-state random binding mechanism and that the rate-limiting step during turnover is decarboxylation and release of α-ketoglutarate (Dean & Koshland, 1993).

The possibility of significant conformational change during turnover was indicated by the behavior of crystals of IDH in the presence of various combinations of substrate, cofactor, and metal ions. The crystals, when soaked with isocitrate/Mg^{2+} or with $NADP^+$ alone, provide excellent quality difference maps which indicate productive substrate binding (Hurley *et al.*, 1990b, 1991). However, when the crystals are soaked with all three components (isocitrate, $NADP^+$, and Mg^{2+}) under otherwise identical conditions, they immediately crack and dissolve, which implies the presence of conformational changes during turnover. Similarly, when crystals of IDH are soaked with isocitrate, $NADP^+$, and calcium rather than magnesium (which virtually eliminates turnover), they are stable and produce difference maps which indicate the formation of an ordered ternary complex. Soaking with α-ketoglutarate, NADPH, and calcium under identical conditions, however, quickly destroys the crystals, leading to the conclusion that the conversion of isocitrate and $NADP^+$ to α-ketoglutarate and NADPH causes a conformational change which should be observable under appropriate conditions.

In order to determine the conformation of IDH which is adopted upon formation of α-ketoglutarate, we have solved the structure of IDH complexed with α-ketoglutarate, NAD-

† This work was supported by National Science Foundation Grant 04200, by Department of Energy Contract No. DE-AC03-76SF00098, and by Markey Charitable Trust support to D.E.K. In addition, B.L.S. was supported by a postdoctoral fellowship from the Helen Hay Whitney Biomedical Sciences Foundation during all the work described in this paper.

‡ Present address: Division of Basic Sciences, Fred Hutchinson Cancer Research Center, 1124 Columbia St., Seattle, WA 98104.

® Abstract published in *Advance ACS Abstracts,* August 15, 1993.

0006-2960/93/0432-9317$04.00/0

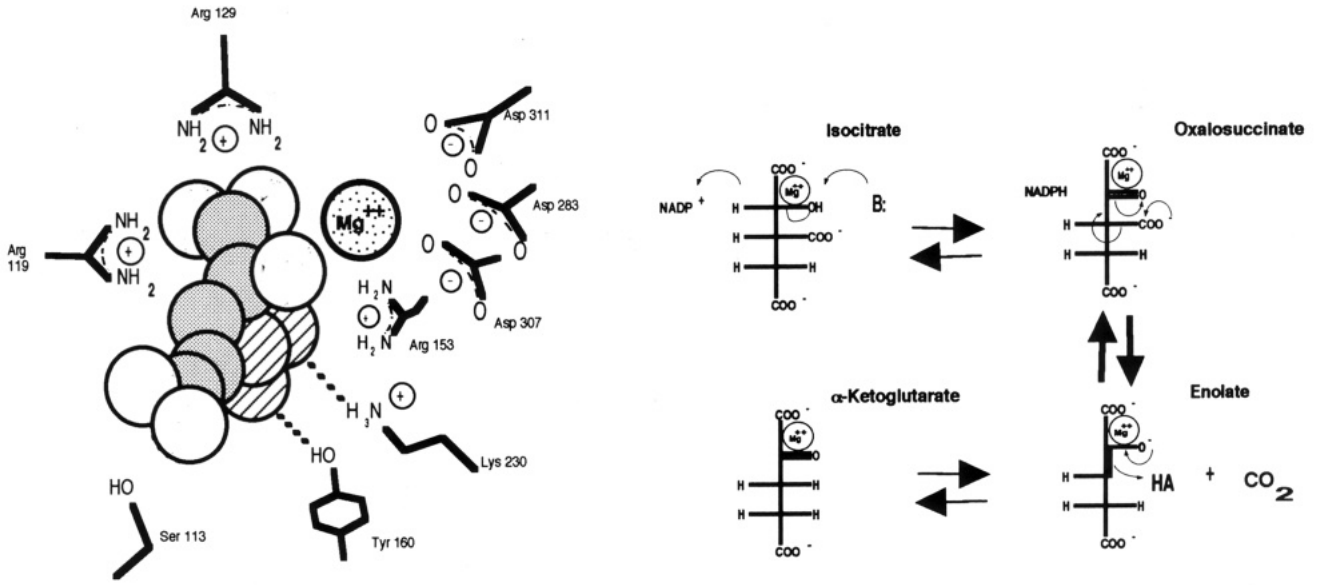

FIGURE 1: Complex of isocitrate in the active site of IDH, with residues involved in substrate binding (Hurley *et al.*, 1990). The labile carboxyl of isocitrate, which is eliminated through a putative endiolate intermediate mechanism to generate α-ketoglutarate and CO_2, is hydrogen bonded to Lys 230′ and Tyr 160.

PH, and Ca^{2+}. Calcium has previously been shown to bind to the enzyme as a complex with either isocitrate or α-ketoglutarate and to cause almost complete inhibition of turnover in both directions as shown by kientic studies (Dean & Koshland, 1993).

MATERIALS AND METHODS

Isocitrate dehydrogenase was purified and crystallized as described (Stoddard *et al.*, 1993). In this case, however, the crystallizations were performed in the presence of α-ketoglutarate, NADPH, and Ca^{2+}, all at concentrations of 150 mM. The drop then equilibrated against a 500-μL reservoir of the ammonium sulfate solution in a tissue culture plate well. The well was sealed with mineral oil. Crystals of 0.3–0.4 mm per side, space group $P4_32_12$, grew within 2 weeks. Characterization of these crystals during data collection and processing showed that the unit cell dimensions were unexpectedly isomorphous with previous crystals of IDH grown in the absence of substrate and cofactor ($a = b = 105.6$ Å, $c = 150.1$ Å). However, the crystals were uniformly smaller and grew at a substantially higher concentration of ammonium sulfate than those from drops prepared in the absence of substrate and cofactor, and they also diffracted to lower resolution (2.7 Å vs 2.5 Å).

Data were collected on an *R*-axis imaging plate area detector with a Rigaku RU-200 rotating-anode X-ray generator operating at 50 kV, 150 mA. Two crystals were used to collect a data set to 2.7-Å resolution using 1° rotations at 10 min/deg. A total of 14 729 reflections (88% of the unique data) were present in the final data set after a 2σ cutoff was applied. The data were processed using the software package RAXIS (Molecular Structure Corp.). The overall R_{merge} between the two crystals was 10.8% on intensities; the overall R_{symm} was 9.5% (see Table I for data statistics). The crystals were extremely unstable in the X-ray beam, necessitating a more rapid pace of data collection, which contributes to the high overall *R*-values for the data; however, these values compare favorably with previously reported data processing statistics for IDH.

Structural Refinement and Map Calculations. Initial difference Fourier maps were calculated prior to refinement, using the coordinates for wild-type IDH (apoenzyme) as previously solved by Hurley *et al.* (1989) and obtained as entry number 1ICD from the Brookhaven Protein Data Bank (Bernstein *et al. 1977*). The strongest featured of this map were the bound α-ketoglutarate and calcium ion and the adenosyl ring of the NADPH. No density was observed for the nicotinamide ring. Also clearly present was difference density representing the movement of the aromatic side chain of tyrosine 160. The coordinates for the enzymes were placed into XPLOR simulated annealing refinement (Brunger *et al.*, 1987) using the structure of uncomplexed isocitrate dehydrogenase as the initial model. No coordinates for substrate, cofactor, metal, or water molecules were included at any stage of these refinements. Refinement was performed against the data set from 10- to 2.7-Å resolution. We used a protocol in which the structure, after the initial static energy minimization, is heated to 4000 °C and then immediately placed into a slow cooling (50 ps) annealing minimization. No extended dynamics were performed during the heat stage of the refinement. Sequential cycles of least-squares refinement were run using

Table I: Data Processing and Refinement Statistics

crystal	1	2
exposure time (h)	5	6.5
rotations (deg)	15	20
radiation-induced decay (%)	28	16
total unique reflections	8078	10 654
overlapping reflections	4003	
Final Data Set and Refinement		
	overall	2.9–2.7 Å
R_{merge}[a] (%)	10.8	14.7
R_{symm}[b] (%)	9.3	13.0
total structure factors	14 729	
resolution (Å)	30–2.7	
refinement *R*-factor[c] (%)	18.5	26.0
Structural Statistics		
total atoms	3880	
bond distance rms (Å)	0.017	
bond angle rms (deg)	3.7	
dihedral rms (deg)	24.3	

[a] Overall *R*-factor between the same reflections from each crystal after scaling, correction for wavelength-dependent absorption, and polarization. $R = \sum_j[I_1(j) - I_2(j)]/\sum_j[I(j)]$. [b] Initial overall *R*-factor (on intensities) between all symmetry-related reflections in the final merged data set.[c] $R = \sum_j|[F_{obs}(j) - F_{calc}(j)]|/\sum_j(F_{obs})$.

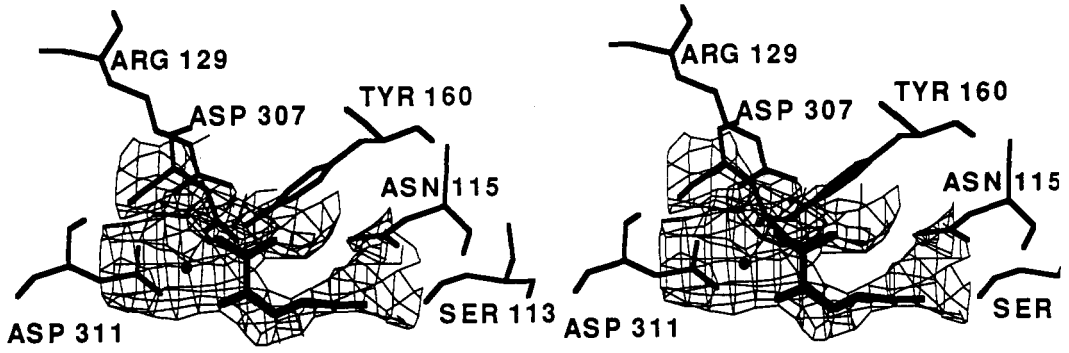

FIGURE 2: Electron density for the bound α-ketoglutarate complex as observed in a $2F_o - F_c$ difference Fourier synthesis. The map was calculated after the initial round of annealing refinement with the protein coordinates only. No coordinates for the bound ternary complex were included in this refinement round or the ensuing phase calculation. The map is contoured at 2σ. The heavy atoms and bonds are shown for the members of the bound complex (α-ketoglutarate and Ca^{2+}) and for neighboring residues. Density is observed for the bound α-ketoglutarate molecule and Ca^{2+} (dark circle) and for several residues exhibiting motions relative to the uncomplexed enzyme but not for the NADPH nicotinamide ring, which is structurally disordered.

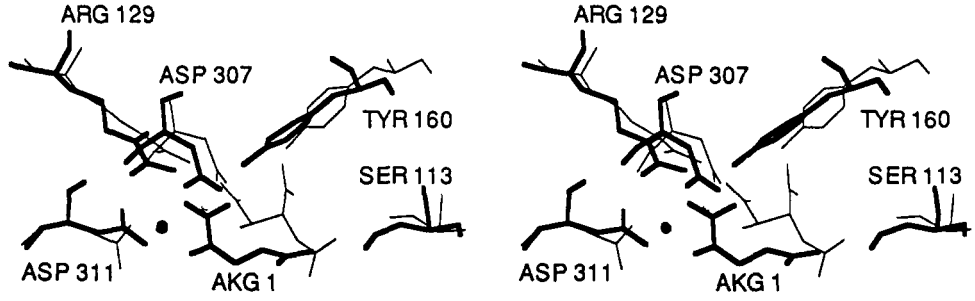

FIGURE 3: Stereo diagram of the active-site-bound, superimposed complexes of α-ketoglutarate (heavy bonds) and isocitrate (light bonds) and the residues involved in binding substrate and metal. Residues from monomer 1 within 3.5 Å of the members of the bound complex are shown. The largest difference between the two structures is seen at tyrosine 160, which is hydrogen-bonded to the labile carboxyl group of isocitrate and moves by over 2 Å in the α-ketoglutarate complex to form a new hydrogen bond to the free side-chain oxygen of Asp 307.

the same initial model. The *R*-factor was 45% initially and 20.0% after convergence.

$F_o - F_c$ difference maps were then recalculated using the coordinates from the refinement to supply phases and calculated structure factors. All the data from 30- to 2.7-Å resolution were included in the map calculation. These maps were examined using the program FRODO (Jones, 1978) on an Evans and Sutherland PS300 graphics display. The largest features in these maps corresponded to the previously solved positions of bound metal, substrate, and the adenine nucleotide of NADPH. No density was observable for the phosphate backbone and nicotinamide ring of the cofactor. The members of the ternary complex were manually built into the structure and the refinement was continued against all the data from 30- to 2.7-Å resolution using XPLOR. With the exception of a pair of active-site water molecules which are complexed to the bound calcium ion, no solvent molecules were included in the final stage of the refinement; also, no heating and annealing was performed. Individual temperature factors were refined for all atoms at the end of the final cycle of refinement, and the values of the temperature factors for the modeled substrate, metal and cofactor atoms were compared to the surrounding protein atoms in the active site. The occupancies were fixed at unity for all atoms. The final structure had an *R*-factor of 18.5% and bond distance rms of 0.017 Å from ideality. The results of the final refinement are shown in Table I.

RESULTS

The structure of the α-ketoglutarate/Ca^{2+}/NADPH complex in the IDH active site clearly differs from the structure of IDH in complex with isocitrate/Mg^{2+} (Hurley *et al.*, 1990b) and also from the structure of IDH in complex with isocitrate/$NADP^+$/Ca^{2+} (Stoddard *et al.*, 1993). Difference maps before and after initial structural refinement show density corresponding to bound α-ketoglutarate and calcium and also to the movement of Tyr 160 and its adjoining residues (Figure 2). The electron density for bound metal and α-ketoglutarate is well formed and can be modeled by a complex of α-ketoglutarate and calcium with small adjustments in torsion angles of the small molecule in the bound complex. The crystallographic electron density for the adenosyl portion of the cofactor and for the bound α-ketoglutarate molecule agree with the positions previously observed in a number of binary complex structures. However, the nicotinamide ring and phosphate backbone of NADPH are unobservable, a result which is similar to the bound structure of $NADP^+$ in the absence of substrate and metal. In contrast, this result is quite different from the structure of the ternary complex of isocitrate, $NADP^+$, and calcium (Stoddard *et al.*, 1993); in that case the cofactor is well-ordered, with electrostatic interactions between the nicotinamide ring nitrogen and the γ-carboxyl of isocitrate causing the cofactor to be structurally ordered and observable. The absence of electron density for the nicotinamide ring in this structure may be due to the absence of attractive electrostatic forces between α-ketoglutarate and NADPH, as compared to the complex of isocitrate and $NADP^+$.

As compared to the structure of the enzyme complexed with isocitrate and magnesium (Hurley *et al.*, 1990b), α-ketoglutarate and calcium are shifted by approximately 1 Å away from serine 113 and toward the conserved aspartic acids (311 and 307) which serve to complex the transition metal (Figure 3). This motion occurs primarily as a rigid body, with the contacts between protein side chains and the carboxylates of α-ketoglutarate maintained in the ternary complex. The hydrogen bond between the γ-carboxylate of α-ketoglutarate and the Ser 113 hydroxyl is maintained, partly

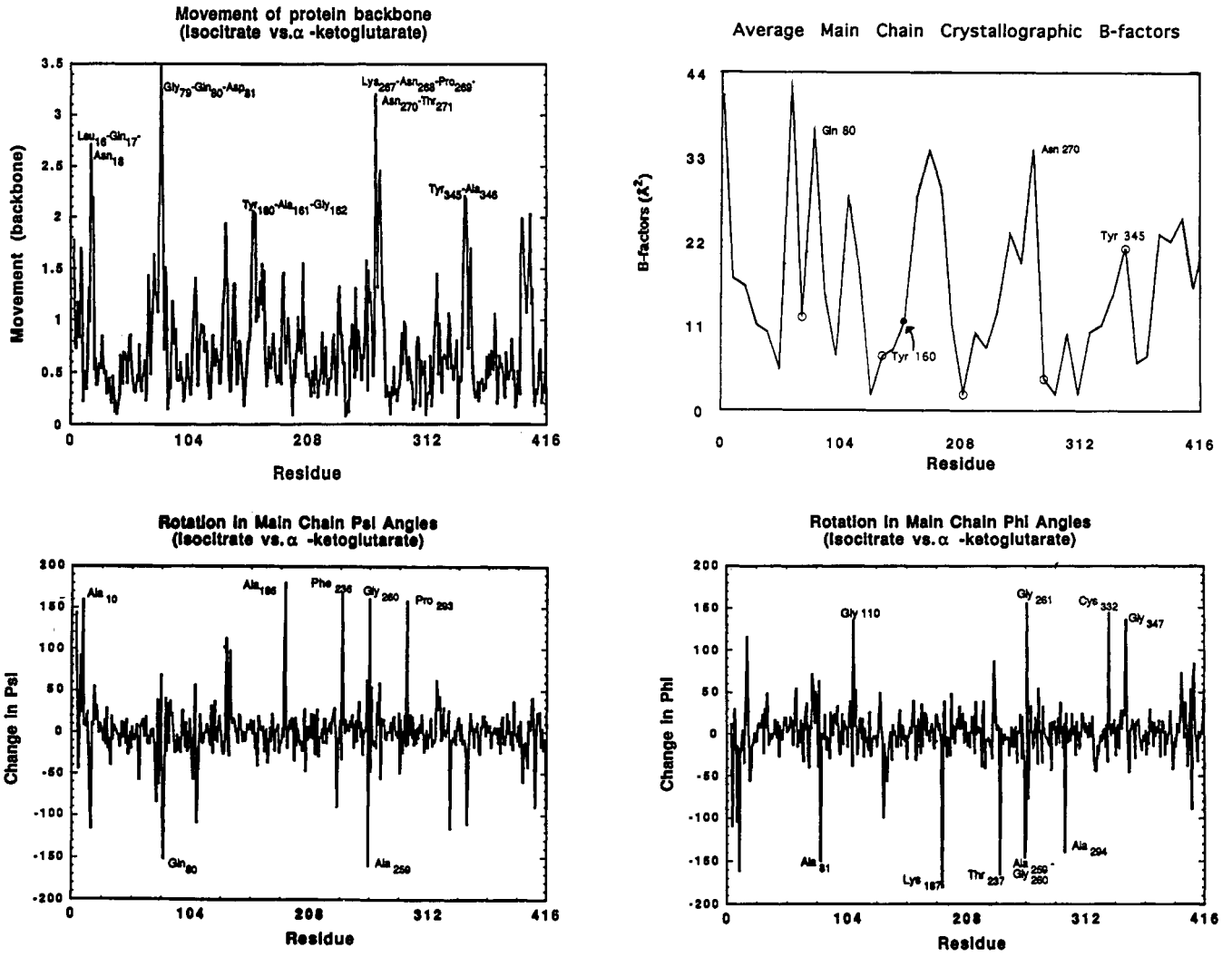

FIGURE 4: Backbone difference plots for isocitrate-bound IDH (Hurley *et al.*, 1990) vs α-ketoglutarate-bound enzyme. The upper left panel shows relative difference between α-carbon positions for the two structures. The lower panels show differences in backbone torsion angles ϕ and φ, respectively. Largest motions are labeled on the graphs. Note the appearance of several sharp pivot points which facilitate the largest motions in protein backbone structure. The α-carbon rms of the two structures is 1.02 Å. The backbone dihedral rms is 18°. The upper right panel displays the average main-chain crystallographic *B*-factors for the IDH monomer. Note that tyrosine 160 is well-ordered in the crystallographic structure but that several of the other regions showing large movements in the difference plots are relatively disordered surface loops (see Figure 5). Nevertheless, the movements observed in the region of the active site are seen to be significant.

by a movement of the serine side chain and backbone by just less than 1 Å. The distance from the α-ketoglutarate hydroxyl oxygen and one of the α-carboxyl oxygens to the bound calcium is 2.9 Å.

Since the bound Ca^{2+} is located approximately 1 Å from the previously solved position of Mg^{2+}, this movement results in an increase in the distance between the metal and the oxygens of isocitrate by 0.5 Å, from the original 2.4 Å in the structure of the Mg^{2+}/isocitrate complex. The movement of the substrate molecule and the bound metal and the increase in metal-to-substrate bond distance were also observed for the ternary complex with isocitrate, $NADP^+$, and calcium and appear to be attributable to the replacement of magnesium with calcium. The Ca^{2+} ion is coordinated by the same protein side chains as magnesium, with bond distances of 2.2–2.4 Å. Two water molecules (which are observed in difference maps) are involved in the metal coordination, and the metal is further coordinated by the α-ketoglutarate hydroxyl oxygen and carboxylate oxygens of aspartates 307 and 283′. Therefore, the main structural effects attributable to calcium that are observed in this structure and in the complex of isocitrate and Ca^{2+} (Stoddard *et al.*, 1993) are (i) a weakened interaction between the bound substrate and the metal and (ii) a movement of the substrate and metal by approximately 1 Å each relative to the isocitrate/magnesium binary complex (Hurley *et al.*, 1990b).

In the current structure of IDH complexed with α-ketoglutarate, however, larger motions of 2–3 Å in the active site and along the adjoining areas of the dimer interface are also observed which are not attributable to the bound calcium but rather appear to be related to the presence of bound α-ketoglutarate and NADPH. These movements are not observed in the structure of IDH complexed with isocitrate and magnesium (Hurley *et al.*, 1990b) or complexed with isocitrate, $NADP^+$, and calcium (Stoddard *et al.*, 1993). Comparison of the substrate (isocitrate) and product (α-ketoglutarate) molecules in complex with the enzyme can shed light on the nature of movements during the catalytic process. The largest structural difference observed in the active site of IDH between the complexes of isocitrate and α-ketoglutarate involves tyrosine 160 (Figures 3 and 4), one of two residues involved in an interaction with the labile carboxyl group of isocitrate which is lost upon conversion to α-ketoglutarate. Upon hydride transfer, decarboxylation, and formation of α-ketoglutarate, this tyrosine side chain and its associated backbone move by over 2 Å in order to form a new hydrogen bond between the tyrosine side chain and the nonbonded side-chain oxygen of Asp 307, a residue which is

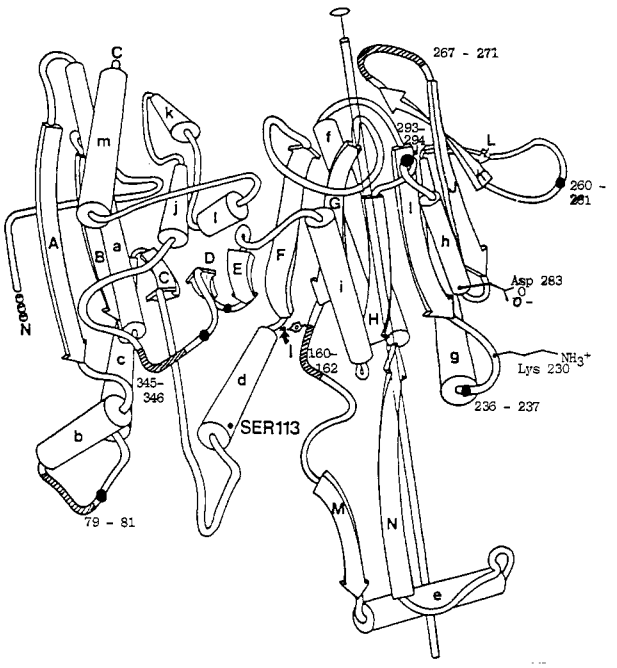

FIGURE 5: Protein fold and regions of greatest movement. Changes in backbone atomic positions over 2 Å are shown with hatching, and locations of dihedral angle changes greater than ±150° are shown by dark circles. The movements at residues 160–162 appear to be directly related to rearrangements in binding patterns in the active site upon decarboxylation of isocitrate, and they influence the overall packing of large areas of secondary structure which participate in dimer formation and the active-site geometry. This specifically includes the mixed α/β motif from residues 220 to 290, which contain a pair of substrate-binding residues from the second subunit of IDH (Lys 230′ and Asp 283′), and which shows movements in backbone positions of 1 Å to over 3 Å in magnitude. The deformation and repacking of this region is accommodated by dihedral torsions in the protein backbone at residues 236–237, 260–261, and 293–294.

also involved in metal chelation. In addition, movements of 0.5–1.5 Å are observed in the protein backbone of large areas of secondary structure flanking the dimer interface and the active site, including residues 230–290 (a region of mixed β-sheet and α-helix), which contain a pair of residues involved in substrate and metal binding (Lys 230′ complexes the carboxyl group which is eliminated during turnover, and Asp 283′ participates in metal binding). This alteration in the packing of secondary structure is manifested to the greatest degree in a movement of the protein backbone of residues 267–271 by over 3 Å, a movement which is facilitated by a large backbone rotation at Gly 260–Gly 261 and Pro 293–Ala 294. The net effect of all these movements appears to be a closure of the active site structure around the 5-carbon decarboxylated product which now contains a planar, sp^2-hybridized C2 carbon and a polar carboxyl group. These movements might reflect the enzyme's binding to the enolate transition state and/or might prevent solvent from participating in unwanted acid/base chemistry. Such a rearrangement to maximize the complementarity of the active site and the substrate molecule is not totally surprising, since the structure of α-ketoglutarate would more closely resemble a postulated enolate transition state of the reaction than the initial isocitrate substrate molecule.

The analysis of this structure shows changes in the position of 2 and 3 Å for several well-ordered protein backbone atoms in the enzyme active site, and more for the side chains (Figures 4 and 5). A small number of large, specific backbone rotations of up to 150° accommodate these movements. Analysis of the data and the refined coordinates (R-factor 18.5% at 2.7-Å resolution with almost 90% of the possible data present) by Wilson plot [$\log(\langle I\rangle/\sum f_j^2)$ vs $4\sin^2\theta/\lambda 2$] and Luzzati plot [R vs $2\sin\theta/\lambda$] shows a maximum uncertainty in the positions of Tyr 160 of 0.5 Å or less, indicating that the largest changes in protein anatomy and atomic positions in the enzyme active site which are induced by binding of α-ketoglutarate as opposed to isocitrate are significant.

DISCUSSION

Induced Fit in IDH and Other Enzymes. The structural changes required to go from the IDH complex with isocitrate to the IDH complex with α-ketoglutarate would require extensive regions of small-scale movement and repacking of secondary structure, culminating in a number of larger movements at the active site and the surrounding dimer interface. These conformational changes may be triggered by the conversion of isocitrate to an intermediate (oxalosuccinate) on the way to the product species (α-ketoglutarate) which has been decarboxylated and contains a new planar carbonyl group at C2. This in turn causes the movement of tyrosine 160 (which is initially hydrogen-bonded to the labile carboxyl of isocitrate) by over 2.5 Å and the formation of a new hydrogen bond to Asp 307. The surrounding backbone region moves toward the bound substrate molecule by a similar distance, forming a tightly packed complex. Further shifts of 0.5–3.2 Å in the backbone positions are observed in a mixed α/β region (consisting of residues 224–290) along the dimer interface. This region contributes a number of residues to the active site from the second subunit, including Asp 283′ and Lys 230′. The slight pivoting movement of this subdomain culminates in a movement of residues 267–271 by 2–3 Å along the protein backbone. The facilitation of the movement of these widely distributed regions of structure within the enzyme can be traced to a small number of well-defined pivot points in the protein backbone.

The magnitude of the changes discussed in this paper is 2–3 Å for backbone atoms and larger for side chains. Wilson and Luzzati plots indicate that the level of uncertainty in atomic positions for these residues is substantially lower than the size of these movements (described in Results section). In addition, the rms differences in Cα positions for this structure vs the isocitrate/Mg^{2+} complex (Hurley *et al.*, 1990b) and the isocitrate/$NADP^+$/Ca^{2+} complex (Stoddard *et al.*, 1993) are much larger at 1.02 and 0.97 Å, respectively, than the corresponding rms between the isocitrate complexes with magnesium and calcium (0.34 Å), which indicates that the changes here are significant and verifiably above background and are produced primarily by the conversion of isocitrate and $NADP^+$ to α-ketoglutarate and NADPH.

Substrate-induced conformational changes in enzymes have been found to be essentially universal and can be categorized in several varieties. A large number display large-scale interdomain closure upon binding of substrate, including hexokinase (Bennett & Steitz, 1980a,b), citrate synthase (Remington *et al.*, 1982; Wiegand *et al.*, 1984), and liver alcohol dehydrogenase (Eklund *et al.*, 1981, 1984). Motions of this sort usually reduce the total surface area of the bound substrate and surrounding active site which is accessible to solvent. This is an important feature in systems which need to avoid the nucleophilic and acid–base reactivity of water. A large number of other enzymes have also been shown to undergo sharp substrate-induced motions which affect smaller, localized loop regions (consisting of a small number of residues) to produce an ordered transition upon binding. The most well studied case of a loop closure is the enzyme triosephosphate isomerase (Phillips *et al.*, 1977; Alber *et al*, 1981; Lolis *et al.*, 1990; Lolis & Petsko, 1990; Joseph *et al.*, 1990). Binding of substrate to TIM induces movement of a 10-residue flexible

loop by as much as 7 Å and serves to prevent water from participating in an undesirable elimination side reaction. Other enzymes which display similar movements upon substrate binding include lactate dehydrogenase (Adams *et al.*, 1970; Grau *et al.*, 1981), H-*ras* ^{21}P (Schlichting *et al.*, 1990; Pai *et al.*, 1990), and malate dehydrogenase (Birktoft *et al.*, 1989). Such movements of distinct loop regions usually occur with little rearrangement of the loop structure itself but instead occur as a pivoting motion of a relatively rigid body around well-defined pivot points.

A separate but closely related family of enzyme conformational motions are those molecules which exhibit local, small-scale movement and deformation of secondary structural elements upon binding of substrate, leading to subtle rearrangements of the active-site environment. Such motions involve smaller changes in the protein's shape and structure than rigid body domain or loop closure. Structural rearrangements of this type are typified by insulin and hemoglobin. In both cases, close-packed α-helices move relative to each other as rigid bodies by 0.5–1.5 Å, utilizing conformational adjustments in the side chains that form the interface between them to accommodate the motion. Such motions, while small in scale, have been shown to play an important role in allosteric conformational changes (such as in hemoglobin) and as the facilitators of even larger movements elsewhere in the molecule, as is observed for citrate synthetase.

Regardless of the specific nature and magnitude of substrate-induced conformational changes in an enzyme's structure, the observed motions can usually be traced back to individual amino acid residues in the active site which participate in bond formation to the moiety that produces the structural change. For example, in citrate synthetase, movement of His 320 and Arg 329 by over 5 Å upon binding citrate produces a 12° rotation of one domain toward the other. In triosephosphate isomerase the displacement of Glu 165 from its hydrogen bond with Ser 96 and its interaction with the substrate molecule triggers the movement of the immediately adjacent residues to close the active site and prevent elimination by solvent. In the case of IDH, the hydride transfer and decarboxylation of isocitrate cause a series of movement in which tyrosine 160 moves to form a new hydrogen bond, which in turn produces a movement of residues 160–163 by over 2 Å and induces a cascade of small movements along the dimer interface and in the active site. Thus, this residue appears to play a key role in decarboxylation and release of α-ketoglutarate.

Isocitrate dehydrogenase illustrates a category of enzyme catalysts which at first would appear to exhibit a templatetype mechanism in which the substrate for the forward reaction (isocitrate) induces few conformational changes, but upon closer inspection the enzyme undergoes catalysis-induced motions which are mechanistically important. It is clear that the conversion of the substrate to product (α-ketoglutarate) induces large conformational changes and that those enzymes that seem to lack substrate-induced conformational changes must be examined structurally at all possible points in their catalytic mechanism.

ACKNOWLEDGMENT

The authors would like to acknowledge the kinetic data and advice which was provided by Drs. Antony Dean and Myoung Lee and the kindness of Dr. Len Banaszak's laboratory members in providing XPLOR parameter and topology files for NADH.

REFERENCES

Adams, M. J., Ford, G. C., Koekok, R., Lentz, P. J., Jr., McPherson, A., Jr., Rossmann, M. G., Smiley, I. E., Schevitz, R. W., & Wonacott, A. J. (1970) *Nature 227*, 1098–1103.

Alber, T., Hartman, F. C., Johnson, R. M., Petsko, G. A., & Tsernoglou, D. (1981) *J. Biol. Chem. 256*, 1356–1361.

Bennett, W. S., & Steitz, T. A. (1980a) *J. Mol. Biol. 140*, 183–209.

Bennett, W. S., & Steitz, T. A. (1980b) *J. Mol. Biol. 140*, 211–230.

Birktoft, J., Rhodes, G., & Banaszak, L. (1989) *Biochemistry 28*, 6065–6081.

Brunger, A. T., Kuriyan, J., & Karplus, M. (1987) *Science 235*, 458.

Dean, A. M., & Koshland, D. E., Jr. (1990) *Science 249*, 1044–1046.

Dean, A. M., & Koshland, D. E., Jr. (1993) *Biochemistry* (first of three papers in this issue).

Eklund, H., Samama, J., Wallen, L., Branden, C., Akeson, A., & Jones, T. (1981) *J. Mol. Biol. 146*, 561–587.

Eklund, H., Samama, J., & Jones, T. (1984) *Biochemistry 23*, 5982.

Grau, U., Trommer, W., and Rossman, M. (1981) *J. Mol. Biol. 151*, 289–307.

Hurley, J. H., Thorsness, P. E., Ramalingam, V., Helmers, N. H., Koshland, D. E., Jr., & Stroud, R. M., (1989) *Proc. Natl. Acad. Sci. U.S.A. 86*, 8635–8639.

Hurley, J. H., Dean, A. M., Sohl, J. L., Koshland, D. E., Jr., & Stroud, R. M. (1990a) *Science 249*, 1012–1016.

Hurley, J. H., Dean, A. M., Thorsness, P. E., Koshland, D. E., Jr., & Stroud, R. M. (1990b) *J. Biol. Chem. 265*, 3599.

Hurley, J. H., Dean, A. M., Koshland, D. E., Jr., & Stroud, R. M. (1991) *Biochemistry 30*, 8671–8678.

Jones, T. A. (1978) *J. Appl. Crystallog. 11*, 268–272.

Joseph, D., Petsko, G. A., and Karplus, M. (1990) *Science 249*, 1425–1428.

Kornberg, H. L., & Madsen, N. B. (1957) *Biochim. Biophys. Acta 24*, 651–653.

LaPorte, D. C., & Koshland, D. E., Jr. (1982) *Nature 300*, 458–460.

LaPorte, D. C., Thorsness, P. E., & Koshland, D. E., Jr. (1985) *J. Biol. Chem. 260*, 10563–10568.

Lolis, E., & Petsko, G. A. (1990) *Biochemistry 29*, 6619–6625.

Lolis, E., Alber, T., Davenport, R. C., Rose, D., Hartman, F. C., & Petsko, G. A. (1990) *Biochemistry 29*, 6609–6618.

Pai, E. F., Krengel, U., Petsko, G. A., Goody, R. S., Kabsch, W., and Wittinghofer, A. (1990) *EMBO J. 9* (8), 2351–2359.

Phillips, D. C., Sternberg, M. J. E., Thornton, J. M., & Wilson, I. A. (1977) *Biochem. Soc. Trans. 12*, 642–647.

Reeves, H. C., Gaston, O. D., Chen, C. L., & Houston, M. (1972) *Biochim. Biophys. Acta 258*, 27–39.

Remington, S., Wiegand, G., & Huber, R. (1982) *J. Mol. Biol. 158*, 111–152.

Schlichting, I., Almo, S. C., Rapp, G., Wilson, K., Petratos, K., Lentfer, A., Wittinghofer, A., Kabsch, W., Pai, E. F., Petsko, G. A., & Goody, R. S. (1990) *Nature 345*, 309–315.

Stoddard, B. L., Dean, A., & Koshland, D. E., Jr. (1993) *Biochemistry* (second of three papers in this issue).

Thorsness, P. E., & Koshland, D. E., Jr. (1987) *J. Biol. Chem. 262*, 10422–10425.

Wiegand, G., Remington, S., Deisenhofer, J., & Huber, R. (1984) *J. Mol. Biol. 174*, 205–219.